

Binary mixture of pseudospin- $\frac{1}{2}$ Bose gases with interspecies spin exchange: from classical fixed points and ground states to quantum ground states

Rukuan Wu^{1,2} and Yu Shi^{1,*}

¹*State Key Laboratory of Surface Physics and Department of Physics, Fudan University, Shanghai 200433, China*

²*Department of Physics, Zhejiang Normal University, Jinhua 321004, China*

We consider the effective spin Hamiltonian describing a mixture of two species of pseudo-spin- $\frac{1}{2}$ Bose gases with interspecies spin exchange. First we analyze the stability of the fixed points of the corresponding classical dynamics, of which the signature is found in quantum dynamics with a disentangled initial state. Focusing on the case without an external potential, we find all the ground states by taking into account quantum fluctuations around the classical ground state in each parameter regime. The nature of entanglement and its relation with classical bifurcation is investigated. When the total spins of the two species are unequal, the maximal entanglement at the parameter point of classical bifurcation is possessed by the excited state corresponding to the classical fixed point which bifurcates, rather than by the ground state.

PACS numbers: 03.75.Mn, 05.45.Mt

I. INTRODUCTION

A remarkable discovery in recent years is that bifurcation in classical dynamics is related to quantum entanglement in the ground state of the corresponding quantum Hamiltonian. In addition to its theoretical demonstration in the Dicke model [1, 2], in a model of two coupled giant spins describing magnetic clusters [3], and in an integrable dimer model [4], this association has also been studied in the area of Bose-Einstein condensation (BEC), including two-component BEC [5, 6] and two-mode atomic-molecular BEC [7, 8]. More recently, a classical bifurcation has been observed in an experiment realizing an internal Josephson effect in a spinor Bose-Einstein condensate, as an important step toward entanglement generation close to critical points [9]. Moreover, in a laser-cooled atom, experimental evidence has been observed for entanglement being a quantum signature of chaos [10].

On the other hand, a novel kind of BEC, the so-called EBEC, that is, BEC of interspecies spin singlet pairs, was found to be the ground state of a Bose system composed of two species of pseudo-spin- $\frac{1}{2}$ Bose atoms with both intraspecies and interspecies spin-exchange interactions in a considerable parameter regime [11–15]. Under the usual single orbital-mode approximation, the Hamiltonian of this system can be transformed into that of two coupled giant spins. Alas, the ground states in all parameter regimes have not yet worked out.

In this paper, we make each of the above two lines of research useful for the other. We focus on the case in the absence of an external potential. First, we study the bifurcation of the classical dynamics corresponding to the Hamiltonian of this Bose mixture, by analyzing the stability of each fixed point. Quantum dynamics

displays some features similar to the classical dynamics if the initial state is a disentangled state, which, however, is not an energy eigenstate. When the numbers of the atoms of the two species are equal, a bifurcation of the fixed points indeed corresponds to a quantum phase transition to a maximally entangled ground state. When they are unequal, the quantum state corresponding to the classical fixed point which bifurcates is also maximally entangled at the bifurcation point. However, it is not the ground state. Finally, we analytically obtain all the quantum ground states by considering quantum fluctuations around the classical ground state in each parameter regime. The analytical results fit the numerical results very well.

The rest of this paper is organized as follows. The model is introduced in Sec. II. The fixed points and bifurcations are studied in Sec. III, with the detailed calculation reported in the Appendix. The classical ground states are described in Sec. IV, and the classical evolution is described in Sec. V, whose quantum analog is described in Sec. VI. Section VII describes the absence of the correspondence between classical bifurcation and maximal entanglement in the case of unequal populations of the two species. In Sec. VIII, we find the quantum ground state in each parameter regime by approximating the Hamiltonian around the classical ground state there. Finally the paper is summarized in Sec. IX.

II. THE MODEL

Consider a dilute gas composed of two distinct species of Bose atoms with the following property [12, 13]. Each atom has an internal degree of freedom represented as a pseudospin- $\frac{1}{2}$, with z -component basis states \uparrow and \downarrow . Under the usual single orbital-mode approximation, for each species α ($\alpha = a, b$) and pseudospin σ ($\sigma = \uparrow, \downarrow$), only the single-particle orbital ground state $\phi_{\alpha\sigma}(\mathbf{r})$ is occupied, then the Hamiltonian can be transformed into that

*Electronic address: yushi@fudan.edu.cn

of two coupled giant spins with spin quantum numbers $S_a = N_a/2$ and $S_b = N_b/2$. Here we focus on the uniform case [14, 15], for which

$$\hat{\mathcal{H}} = J_{\perp}(\hat{S}_{ax}\hat{S}_{bx} + \hat{S}_{ay}\hat{S}_{by}) + J_z\hat{S}_{az}\hat{S}_{bz} \quad (1)$$

where $J_{\perp} = 4\pi\hbar^2\xi_e/(m_{ab}\Omega)$ while $J_z = 4\pi\hbar^2(\xi_s - \xi_d)/(m_{ab}\Omega)$, with m_{ab} being the reduced mass of an a atom and a b atom, ξ_e is the scattering length for the scattering in which an a atom and a b atom exchange pseudospins, ξ_s being the scattering length for the forward scattering in which an a atom and a b atom have different pseudospins without spin exchange, ξ_d being the scattering length for the forward scattering in which an a atom and a b atom have the same pseudospin without spin exchange, Ω being the volume of the system, $\hat{\mathbf{S}}_{\alpha} = \hat{a}_{\sigma}^{\dagger}\mathbf{s}_{\sigma\sigma'}\hat{a}_{\sigma'}$, $\mathbf{s}_{\sigma\sigma'}$ is the single spin operator, α_{σ} denotes the annihilation operator associated with $\phi_{\alpha\sigma}(\mathbf{r})$ of species α . Without loss of generality, suppose $S_a \geq S_b$.

The corresponding classical Hamiltonian is obtained from (1) by treating the spin operators as the classical spin variables,

$$\mathcal{H}_{cl} = J_{\perp}(S_{ax}S_{bx} + S_{ay}S_{by}) + J_zS_{az}S_{bz} \quad (2)$$

$$= J_{\perp}\sqrt{(S_a^2 - S_{az}^2)(S_b^2 - S_{bz}^2)}\cos(\varphi_a - \varphi_b) + J_zS_{az}S_{bz} \quad (3)$$

From the Hamiltonian (1), one obtains the equations of motion

$$\begin{aligned} \frac{d\hat{S}_{\alpha x}}{dt} &= J_{\perp}\hat{S}_{\alpha z}\hat{S}_{\beta y} - J_z\hat{S}_{\alpha y}\hat{S}_{\beta z}, \\ \frac{d\hat{S}_{\alpha y}}{dt} &= -J_{\perp}\hat{S}_{\alpha z}\hat{S}_{\beta x} + J_z\hat{S}_{\alpha x}\hat{S}_{\beta z}, \\ \frac{d\hat{S}_{\alpha z}}{dt} &= J_{\perp}(\hat{S}_{\alpha y}\hat{S}_{\beta x} - \hat{S}_{\alpha x}\hat{S}_{\beta y}). \end{aligned} \quad (4)$$

The corresponding classical equations of motion, obtained either from the classical Hamiltonian (2) or from the quantum equations of motion by replacing the spin operators as the classical spin variables, can be written as

$$\frac{d\mathbf{A}}{dt} = \mathcal{J}\mathbf{A}, \quad (5)$$

where $\mathbf{A} \equiv (S_{ax}, S_{ay}, S_{az}, S_{bx}, S_{by}, S_{bz})^T$,

$$\mathcal{J} \equiv \begin{pmatrix} 0 & -J_zS_{bz} & J_{\perp}S_{by} & 0 & J_{\perp}S_{az} & -J_zS_{ay} \\ J_zS_{bz} & 0 & -J_{\perp}S_{bx} & -J_{\perp}S_{az} & 0 & J_zS_{ax} \\ -J_{\perp}S_{by} & J_{\perp}S_{bx} & 0 & J_{\perp}S_{ay} & -J_{\perp}S_{ax} & 0 \\ 0 & J_{\perp}S_{bz} & -J_zS_{by} & 0 & -J_zS_{az} & J_{\perp}S_{ay} \\ -J_{\perp}S_{bz} & 0 & J_zS_{bx} & J_zS_{az} & 0 & -J_{\perp}S_{ax} \\ J_{\perp}S_{by} & -J_{\perp}S_{bx} & 0 & -J_{\perp}S_{ay} & J_{\perp}S_{ax} & 0 \end{pmatrix}.$$

In studying the stability of a fixed point, \mathcal{J} becomes the Jacobian matrix when the spin variables adopt the values at this fixed point.

The classical Hamiltonian in the form of (3) suggests that the classical state of the system is completely determined by the variables S_{az} , S_{bz} , and $\varphi_a - \varphi_b$.

We shall use (3) studying the evolution in Sec. V, while using (2) in analyzing the fixed points in Sec. III, because there is arbitrariness of angles ϕ_a and ϕ_b in some fixed points.

III. FIXED POINTS AND BIFURCATIONS IN CLASSICAL DYNAMICS

The fixed points of the classical dynamics are obtained from

$$\frac{d\mathbf{A}}{dt} = 0. \quad (6)$$

The stability of each fixed point can be examined first by studying the eigenvalues of Jacobian matrix \mathcal{J} at this point: It is stable if every eigenvalue has a negative real part, while it is unstable if any eigenvalue has a positive real part. Otherwise, one cannot judge whether the fixed point is stable from the eigenvalues of \mathcal{J} , but it is certainly stable if a Lyapunov function can be constructed. A Lyapunov function \mathcal{F} is such that in a neighborhood of the fixed point, \mathcal{L} is minimal (or maximal) at the fixed point, and $d\mathcal{L}/dt \leq 0$ (or $d\mathcal{L}/dt \geq 0$).

There exist eight fixed points in our system. Their stability is analyzed in the Appendix. The stable parameter regimes of these fixed points are shown in Fig.1. We specify the fixed point in terms of direction \mathbf{n}_{α} of the spin vector $\mathbf{S}_{\alpha} = S_{\alpha}\mathbf{n}_{\alpha}$, that is, $\mathbf{n}_{\alpha} \equiv (\sin\theta_{\alpha}\cos\varphi_{\alpha}, \sin\theta_{\alpha}\sin\varphi_{\alpha}, \cos\theta_{\alpha})$, with $0 \leq \theta_{\alpha} \leq \pi$, $0 \leq \varphi_{\alpha} < 2\pi$, $\alpha = a, b$.

As shown in FIG. 1, the fixed points and their stable regimes are the following.

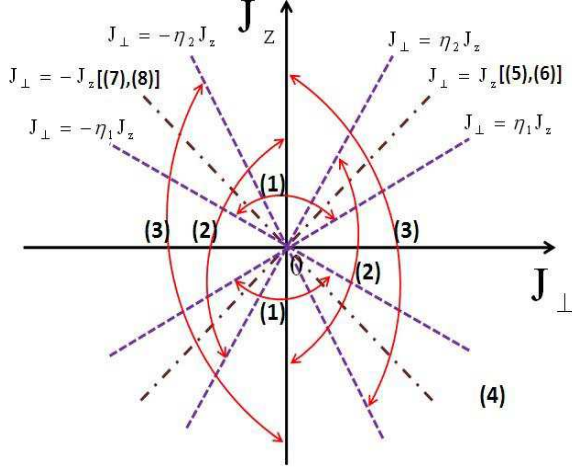


FIG. 1: (Color online) The stable parameter regimes of the fixed points on $J_{\perp} - J_z$ plane. The fixed points are (1) $\mathbf{n}_a = -\mathbf{n}_b = (0, 0, 1)$ or $\mathbf{n}_a = -\mathbf{n}_b = (0, 0, -1)$, (2) $\mathbf{n}_a = -\mathbf{n}_b = (\cos \varphi, \sin \varphi, 0)$, (3) $\mathbf{n}_a = \mathbf{n}_b = (\cos \varphi, \sin \varphi, 0)$, (4) $\mathbf{n}_a = \mathbf{n}_b = (0, 0, 1)$ or $\mathbf{n}_a = \mathbf{n}_b = (0, 0, -1)$, (5) $\mathbf{n}_a = \mathbf{n}_b$, (6) $\mathbf{n}_a = -\mathbf{n}_b$, (7) $\mathbf{n}_a = (\sin \theta \cos \varphi, \sin \theta \sin \varphi, \cos \theta)$, while $\mathbf{n}_b = (\sin \theta \cos \varphi, \sin \theta \sin \varphi, -\cos \theta)$, (8) $\mathbf{n}_a = (\sin \theta \cos \varphi, \sin \theta \sin \varphi, \cos \theta)$, while $\mathbf{n}_b = (-\sin \theta \cos \varphi, -\sin \theta \sin \varphi, \cos \theta)$. The fixed point (4) is always stable, which the stable regimes of the other fixed points are indicated by using the curves with arrows at both ends.

(1) $\mathbf{n}_a = -\mathbf{n}_b = (0, 0, \pm 1)$. One spin is the parallel to the z direction while the other is antiparallel to the z direction. This fixed point is stable when $\eta_1 |J_z| > |J_{\perp}|$, where $\eta_1 \equiv \frac{1}{2} \left(\sqrt{\frac{S_a}{S_b}} + \sqrt{\frac{S_b}{S_a}} \right)$.

(2) $\mathbf{n}_a = -\mathbf{n}_b = (\cos \varphi, \sin \varphi, 0)$, where $0 \leq \varphi < 2\pi$. The two spins are antiparallel and are both on the $x - y$ plane. This fixed point is stable if $J_{\perp} > 0$ and $J_{\perp} > \eta_2 J_z$, or $J_{\perp} < 0$ and $J_{\perp} < \eta_2 J_z$, where $\eta_2 \equiv \frac{2S_a S_b}{S_a^2 + S_b^2}$.

(3) $\mathbf{n}_a = \mathbf{n}_b = (\cos \varphi, \sin \varphi, 0)$. The two spins are parallel and are on the $x - y$ plane. This fixed point is stable when $J_{\perp} > 0$ and $J_{\perp} > -\eta_2 J_z$, or $J_{\perp} < 0$ and $J_{\perp} < -\eta_2 J_z$.

(4) $\mathbf{n}_a = \mathbf{n}_b = (0, 0, \pm 1)$. The two spins are both parallel or antiparallel to the z direction. This fixed point is always stable.

(5) $\mathbf{n}_a = -\mathbf{n}_b$. The two spins are always antiparallel. This fixed point only exists at $J_{\perp} = J_z$ and is stable.

(6) $\mathbf{n}_a = \mathbf{n}_b$. The two spins are always parallel. This fixed point only exists at $J_{\perp} = J_z$ and is stable.

(7) $\mathbf{n}_a = (\sin \theta \cos \varphi, \sin \theta \sin \varphi, \cos \theta)$ while $\mathbf{n}_b = (\sin \theta \cos \varphi, \sin \theta \sin \varphi, -\cos \theta)$. The z components of the two spins are opposite. This fixed point only exists at $J_{\perp} = -J_z$ and is stable.

(8) $\mathbf{n}_a = (\sin \theta \cos \varphi, \sin \theta \sin \varphi, \cos \theta)$ while $\mathbf{n}_b = (-\sin \theta \cos \varphi, -\sin \theta \sin \varphi, \cos \theta)$. The xy components of the two spins are opposite. This fixed point only exists at $J_{\perp} = -J_z$ and is stable.

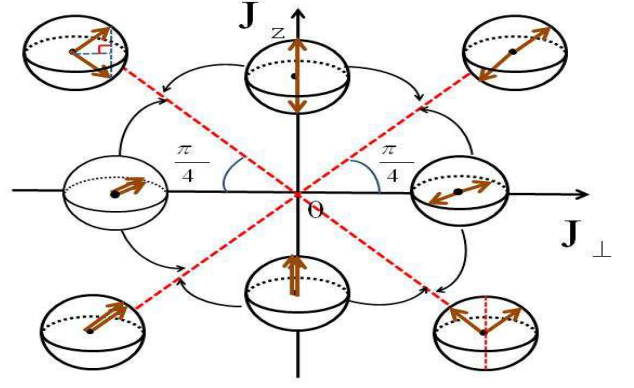


FIG. 2: (Color online) Classical ground states in different regimes of parameters J_{\perp} and J_z . They are just the eight fixed points, but there are differences in the parameter regimes although there are overlaps. (i) $J_z > |J_{\perp}|$, the fixed point (1); (ii) $J_{\perp} > |J_z|$, the fixed point (2); (iii) $J_{\perp} < -|J_z|$, the fixed point (3); (iv) $J_z < -|J_{\perp}|$, the fixed point (4); (v) $J_{\perp} = J_z > 0$, the fixed point (5); (vi) $J_{\perp} = J_z < 0$, the fixed point (6); (vii) $J_{\perp} = -J_z > 0$, the fixed point (7); (viii) $J_{\perp} = -J_z < 0$, the fixed point (8).

It can be seen that $J_{\perp} = \pm \eta_1 J_z$ and $J_{\perp} = \pm \eta_2 J_z$ are bifurcation points.

IV. CLASSICAL GROUND STATES

As depicted in Fig. 2, it can be found that classically the energy is minimal at fixed point (1) when $J_z > |J_{\perp}|$; at fixed point (2) when $J_{\perp} > |J_z|$; at fixed point (3) when $J_{\perp} < -|J_z|$; at fixed point (4) when $J_z < -|J_{\perp}|$; at fixed point (5) when $J_{\perp} = J_z > 0$; at fixed point (6) when $J_{\perp} = J_z < 0$; at fixed point (7) when $J_{\perp} = -J_z > 0$; at fixed point (8) when $J_{\perp} = -J_z < 0$.

If $S_a = S_b$, we have $\eta_1 = \eta_2 = 1$; therefore the parameter regimes of the bifurcation points are completely the same as those of the classical ground states, respectively. But if $S_a \neq S_b$, there are differences although there are overlap regimes.

V. CLASSICAL EVOLUTION

Because the Hamiltonian conserves $S_{az} + S_{bz}$, we study the dynamical evolution of $S_{az} - S_{bz}$ and $(\varphi_a - \varphi_b)/2$ for some given values of $S_{az} + S_{bz}$. When $S_{az} = S_a$ while $S_{bz} = S_b$, or $S_{az} = -S_a$ while $S_{bz} = -S_b$, the system is at the fixed point (1). When $S_{az} = 0$, $S_{bz} = 0$ while $(\varphi_a - \varphi_b)/2 = \pi/2$, the system is at the fixed point (2). When $S_{az} = 0$, $S_{bz} = 0$ while $(\varphi_a - \varphi_b)/2 = 0$ or π , the system is at the fixed point (3).

We have studied the evolution trajectories near fixed points (1), (2) and (3) under various values of $S_a = S_b$. As shown in Fig. 3, when $J_{\perp}/J_z < 1$, fixed points (1)

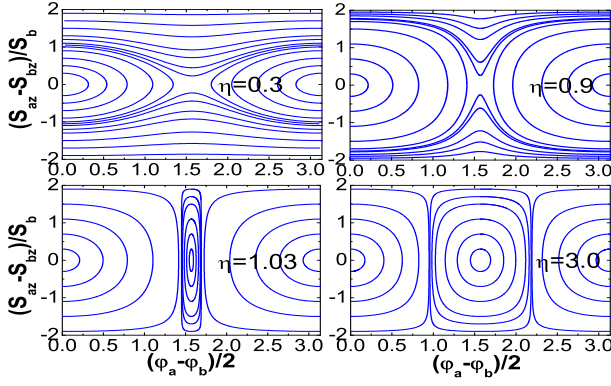


FIG. 3: (Color online) The evolution trajectories on the plane of $(S_{az} - S_{bz})/S_b$ and $(\varphi_a - \varphi_b)/2$, for various values of $S_a = S_b$. Here $\eta \equiv J_{\perp}/J_z$, $S_{az} + S_{bz} = 0$.

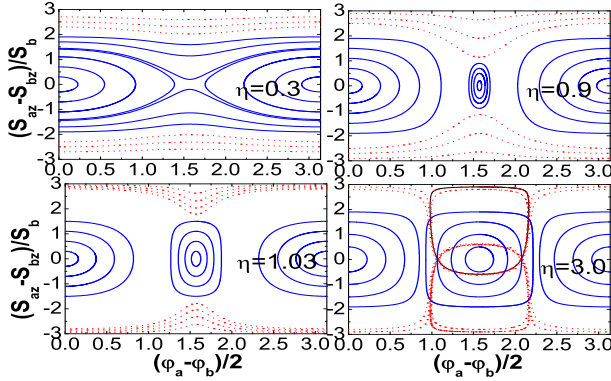


FIG. 4: (Color online) The evolution trajectories on the plane of $(S_{az} - S_{bz})/S_b$ and $(\varphi_a - \varphi_b)/2$, for various values of $S_a = 2S_b$. Here $\eta \equiv J_{\perp}/J_z$. The solid lines describe the dynamics for $S_{az} + S_{bz} = 0$ and the dot lines describe the dynamics for $S_{az} + S_{bz} = \pm(S_a - S_b)$.

and (3) are stable while fixed point (2) is unstable; when $J_{\perp}/J_z > 1$, fixed points (2) and (3) are stable while fixed point (1) is unstable. This conclusion is reached by considering that a fixed point is stable if the evolution trajectories are loops around a fixed point, otherwise it is unstable.

We have also studied the case of $S_a \neq S_b$. As shown in Fig. 4 for $S_a = 2S_b$, the evolution trajectories are different from the case of $S_a = S_b$. For $J_{\perp}/J_z = 0.9$ and for $J_{\perp}/J_z = 1.03$, three fixed points are all stable.

Note that all the results of the numerical simulation are consistent with the above theoretical analysis.

VI. QUANTUM EVOLUTION WITH DISENTANGLED INITIAL STATE

To simulate a quantum process closest to classical evolution, we choose as the initial state a disentangled state,

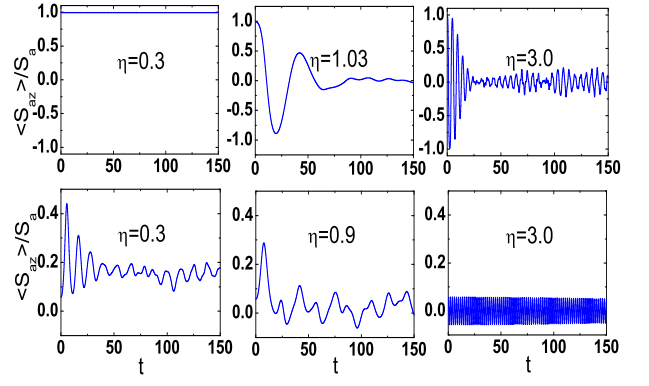


FIG. 5: (Color online) Quantum dynamics of $\langle S_{az} \rangle / S_a$ for $S_a = S_b = 300$ and various values of $\eta \equiv J_{\perp}/J_z$. The figures on the upper line exhibit the stability of fixed point (1). The figures on the second line exhibit the stability of fixed point (2). The unit of t is $1/J_z$.

which can always be written as

$$\begin{aligned}
 |\psi\rangle &= (e^{-i\varphi_a/2} \cos \frac{\theta_a}{2} |\uparrow\rangle_a + e^{i\varphi_a/2} \sin \frac{\theta_a}{2} |\downarrow\rangle_a)^{N_a} \\
 &\otimes (e^{-i\varphi_b/2} \cos \frac{\theta_b}{2} |\uparrow\rangle_b + e^{i\varphi_b/2} \sin \frac{\theta_b}{2} |\downarrow\rangle_b)^{N_b} \quad (7) \\
 &= |S_a \mathbf{n}_a\rangle \otimes |S_b \mathbf{n}_b\rangle.
 \end{aligned}$$

where $|\uparrow\rangle_{\alpha}$ denotes the spin state of a single atom of species α , while $|S_{\alpha} \mathbf{n}_{\alpha}\rangle$ represents the state of the total spin of species α . In this state, the spin components of each species are similar to classical spins; that is, $\langle \hat{S}_{\alpha x} \rangle = S_{\alpha} \sin \theta_{\alpha} \cos \varphi_{\alpha}$, $\langle \hat{S}_{\alpha y} \rangle = S_{\alpha} \sin \theta_{\alpha} \sin \varphi_{\alpha}$, and $\langle \hat{S}_{\alpha z} \rangle = S_{\alpha} \cos \theta_{\alpha}$ ($\alpha = a, b$). Moreover, we choose θ_{α} and φ_{α} in such a way that $\langle \hat{S}_{\alpha} \rangle$ corresponds to a fixed point in classical dynamics. For fixed point (1), $\mathbf{n}_a = -\mathbf{n}_b = (0, 0, 1)$; thus the initial state is $|\psi_{(1)}\rangle = |\uparrow\rangle_a^{\otimes N_a} |\downarrow\rangle_b^{\otimes N_b}$. For fixed point (2), $\mathbf{n}_a = -\mathbf{n}_b = (\cos \varphi, \sin \varphi, 0)$; thus the initial state is $|\psi_{(2)}\rangle = (\frac{1}{\sqrt{2}} e^{-i\varphi/2} |\uparrow\rangle_a + \frac{1}{\sqrt{2}} e^{i\varphi/2} |\downarrow\rangle_a)^{\otimes N_a} (\frac{-i}{\sqrt{2}} e^{-i\varphi/2} |\uparrow\rangle_b + \frac{i}{\sqrt{2}} e^{i\varphi/2} |\downarrow\rangle_b)^{\otimes N_b}$. This is so because $\hat{S}_{\alpha z} = \hat{N}_{\alpha\uparrow} - \frac{N_{\alpha}}{2} = \frac{N_{\alpha}}{2} - \hat{N}_{\alpha\downarrow}$, where $\hat{N}_{\alpha\sigma}$ is the number of atoms of species α with spin σ ($\alpha = a, b$; $\sigma = \uparrow, \downarrow$).

For each initial state $|\psi\rangle$ in the form of (7), we evaluate

$$\langle \hat{S}_{\alpha z}(t) \rangle = \langle \psi | e^{i\hat{H}t} \hat{S}_{\alpha z} e^{-i\hat{H}t} | \psi \rangle, \quad (8)$$

whose evolution actually represents the change of the distribution of the atoms of species α in the two pseudospin states.

We choose the same initial conditions as in the classical case in last section to start the quantum dynamics. It is found that the classification of the stability of the classical dynamics still applies. The result is shown in Fig. 5 for the case of $S_a = S_b$, and in Fig. 6 for the case of $S_a = 2S_b$.

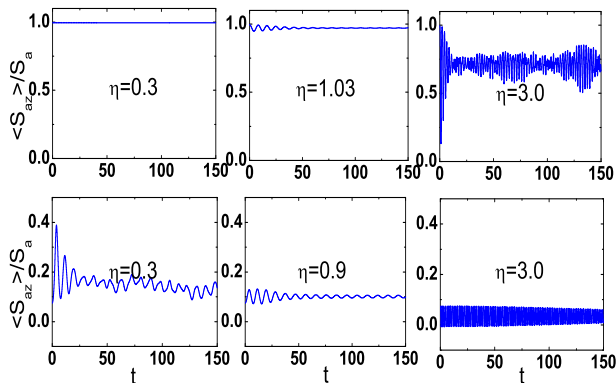


FIG. 6: (Color online) Quantum dynamics of $\langle S_{az} \rangle / S_a$ for $S_a = 2S_b = 300$ and various values of $\eta \equiv J_{\perp} / J_z$. The figures on the upper line exhibit the stability of fixed point (1). The figures on the second line exhibit the stability of fixed point (2). The unit of t is $1/J_z$.

The reason why quantum dynamics under the disentangled initial state is so close to classical one is the following. In Heisenberg picture, the quantum equations of motion (4) reduce to the classical ones (5), with $\langle S_{\alpha i} \rangle$, ($i = x, y, z$), substituting the corresponding classical spin variable.

VII. BIFURCATION AND ENTANGLEMENT

The ground state can always be written as $|G_{S_z}\rangle = \sum f(m, S_z) |S_a, m\rangle_a |S_b, S_z - m\rangle_b$, where the interspecies entanglement can be quantified as $-\sum_m f^2(m, S_z) \log_2 S_b + 1 f^2(m, S_z)$ [12]. It has been shown that when $S_a = S_b = S$, the entanglement of the ground state is maximal at $J_{\perp} = J_z$, where the ground state is $(\sqrt{2S+1})^{-1} \sum_{m=-S}^S (-1)^m |S, m\rangle_a |S, -m\rangle_b$ [12]. Using the transformation $U = e^{i\pi S_{bz}}$, we can obtain the ground state at $J_{\perp} = -J_z$ as $(\sqrt{2S+1})^{-1} \sum_{m=-S}^S |S_a, m\rangle_a |S_b, -m\rangle_b$, which is also maximally entangled.

When $S_a = S_b$, there is only one bifurcation point at $J_{\perp} = J_z$ between the fixed points (1) and (2); there is also only one bifurcation point at $J_{\perp} = -J_z$ between the fixed points (1) and (3). Each of these bifurcation points corresponds to a maximally entangled quantum ground state.

However, when $S_a \neq S_b$, $\eta_1 \neq \eta_2$, there are two bifurcation points $J_{\perp} = \eta_1 J_z$ and $J_{\perp} = \eta_2 J_z$ between the fixed points (1) and (2). Similarly, there are two bifurcation points $J_{\perp} = -\eta_1 J_z$ and $J_{\perp} = -\eta_2 J_z$ between the fixed points (1) and (3).

Numerical calculations indicate that in consistency with the classical ground states, the total z -component spin exhibits the following features. When $J_z > 0$ while $\eta < 1$, $S_z = \pm(S_a - S_b)$. When $J_z > 0$ while $\eta > 1$, $S_z = p$, with $p = 0$ if $S_a - S_b$ is an integer while $p = \pm 1/2$

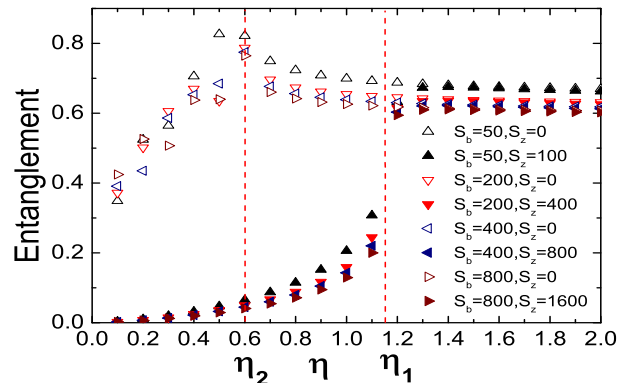


FIG. 7: (Color online) The numerical result of the entanglement entropy of the quantum states of $S_z = 0$ and $S_z = S_a - S_b$, as a function of η . Here $S_a = 3S_b$, $J_z > 0$.

if $S_a - S_b$ is a half integer.

Numerical results of the entanglement entropy of the states with $S_z = S_a - S_b$ and $S_z = 0$, varying with η , are shown in Fig.7 for some integer values of S_b and $S_a = 3S_b$. For $\eta < 1$, the ground state is the one with $S_z = S_a - S_b$, whose entanglement values are plotted as empty triangles. For $\eta > 1$, the ground state is the one with $S_z = 0$, whose entanglement values are plotted as filled triangles. Therefore, there is a discontinuity of entanglement in passing $\eta = 1$, where both states are degenerate ground states.

According to the bifurcation analysis discussed above, when $S_a = 3S_b$, the two bifurcation points are $\eta_1 = \frac{1}{2}(\sqrt{1/3} + \sqrt{3}) \approx 1.1547$ and $\eta_2 = 0.6$. As indicated in FIG.7, the entanglement entropy of the states with $S_z = 0$ and $S_z = S_a - S_b$ is maximal at η_1 and η_2 , respectively, and decreases rapidly in deviating from each of them, with the decrease more rapid for η larger than the maximal point.

Therefore, when $S_a \neq S_b$, the quantum state corresponding to each classical fixed point still possesses maximal entanglement at the parameter point where the fixed point bifurcates. However, this quantum state is not the quantum ground state. In other words, the entanglement of the quantum ground state at each bifurcation point is not maximal anymore.

VIII. ANALYTICAL SOLUTIONS OF THE QUANTUM GROUND STATES

We now proceed to analytically find out the quantum ground states on all $J_{\perp} - J_z$ parameter regimes, by using effective Hamiltonians which describe deviations from the classical ground state in each parameter regime. All the ground states are summarized in Fig. 8. Regimes A ($J_z > |J_{\perp}|$) and B ($J_z < -|J_{\perp}|$) both correspond to $|\xi_s - \xi_d| > |\xi_e|$; i.e., the interspecies spin exchange scattering is quite weak, with A and B differing

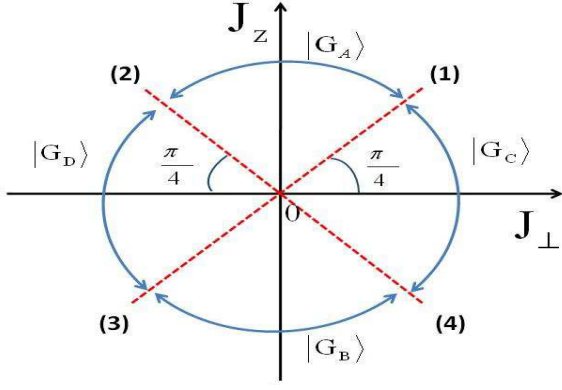


FIG. 8: (Color online) The quantum ground states in all the parameter regimes. $|G_i\rangle$ ($i = A, B, C, D$) represent the ground states in the four bulk regimes, and are given in Secs. VIIIA to VIIID. (1) to (4) represent the four boundaries, in which the ground states are described in Sec. VIIIE.

in whether the equal-spin forward scattering length is larger or smaller than the unequal-spin forward scattering length. Regimes C ($J_\perp > |J_z|$) and D ($J_\perp < -|J_z|$) both correspond to $|\xi_e| > |\xi_s - \xi_d|$; i.e., the interspecies spin exchange scattering is quite strong, with C and D differing in whether the spin-exchange scattering length is positive or negative.

Regime A ($J_z > J_\perp$) corresponds to $\xi_s - \xi_d > |\xi_e|$; i.e., the interspecies spin exchange scattering is quite weak.

A. $J_z > |J_\perp|$

As shown in Fig. 2, in this parameter regime, the classical ground state is fixed point (1), i.e., $|S_a, S_a\rangle|S_b, -S_b\rangle$ or $|S_a, -S_a\rangle|S_b, S_b\rangle$.

First we consider the quantum ground state near $|S_a, S_a\rangle|S_b, -S_b\rangle$. One can make the Holstein-Primarkoff transformation [16],

$$\begin{aligned}\hat{S}_{a-} &= \hat{f}_a^\dagger \sqrt{2S_a - \hat{f}_a^\dagger \hat{f}_a}, & \hat{S}_{a+} &= \sqrt{2S_a - \hat{f}_a^\dagger \hat{f}_a} \hat{f}_a, \\ \hat{S}_{az} &= S_a - \hat{f}_a^\dagger \hat{f}_a, \\ \hat{S}_{b-} &= \sqrt{2S_b - \hat{f}_b^\dagger \hat{f}_b} \hat{f}_b, & \hat{S}_{b+} &= \hat{f}_b^\dagger \sqrt{2S_b - \hat{f}_b^\dagger \hat{f}_b}, \\ \hat{S}_{bz} &= \hat{f}_b^\dagger \hat{f}_b - S_b,\end{aligned}\quad (9)$$

with $\hat{S}_{\alpha\pm} \equiv \hat{S}_{ax} \pm i\hat{S}_{ay}$, $\alpha = a, b$, \hat{f}_α and \hat{f}_α^\dagger being bosonic operators satisfying $\hat{f}_\alpha |n_\alpha\rangle = \sqrt{n_\alpha} |n_\alpha - 1\rangle$, $\hat{f}_\alpha^\dagger |n_\alpha\rangle = \sqrt{n_\alpha + 1} |n_\alpha + 1\rangle$, $[\hat{f}_\alpha, \hat{f}_\beta] = 0$, $[\hat{f}_\alpha, \hat{f}_\beta^\dagger] = \delta_{\alpha\beta}$, where

$$|n_a\rangle \equiv |S_a, S_a - n_a\rangle_a, \quad (10)$$

$$|n_b\rangle \equiv |S_b, -S_b + n_b\rangle_b, \quad (11)$$

$n_\alpha = 0, 1, 2, \dots, 2S_\alpha$. When S_α is very large, $\langle \hat{f}_\alpha^\dagger \hat{f}_\alpha \rangle \ll 2S_\alpha$, $\hat{S}_{\alpha-} \approx (2S_\alpha)^{1/2} \hat{f}_\alpha^\dagger$, $\hat{S}_{az} \hat{S}_{bz} \approx S_b \hat{f}_a^\dagger \hat{f}_a + S_a \hat{f}_b^\dagger \hat{f}_b - S_a S_b$. Then the Hamiltonian (1) can be approximated as

$$\begin{aligned}\hat{\mathcal{H}} &\approx -J_z S_a S_b + J_z (S_b \hat{f}_a^\dagger \hat{f}_a + S_a \hat{f}_b^\dagger \hat{f}_b) \\ &\quad + J_\perp \sqrt{S_a S_b} (\hat{f}_a^\dagger \hat{f}_b^\dagger + \hat{f}_b \hat{f}_a),\end{aligned}\quad (12)$$

Then we make the Bogoliubov transformation

$$\begin{aligned}\hat{f}_c &= \sqrt{\frac{\Delta_1 + 1}{2}} \hat{f}_a + \text{sgn}(J_\perp) \sqrt{\frac{\Delta_1 - 1}{2}} \hat{f}_b^\dagger, \\ \hat{f}_d &= \text{sgn}(J_\perp) \sqrt{\frac{\Delta_1 - 1}{2}} \hat{f}_a^\dagger + \sqrt{\frac{\Delta_1 + 1}{2}} \hat{f}_b,\end{aligned}\quad (13)$$

where $\text{sgn}(J_\perp)$ is the sign of J_\perp , $\Delta_1 \equiv \frac{J_z(S_a + S_b)}{\sqrt{J_z^2(S_a + S_b)^2 - 4J_\perp^2 S_a S_b}}$. When $S_a = S_b$ and $J_z = J_\perp$, $\Delta_1 \pm 1$ should be 1. Hamiltonian(12) becomes

$$\hat{\mathcal{H}}_A = \epsilon_{1c} \hat{f}_c^\dagger \hat{f}_c + \epsilon_{1d} \hat{f}_d^\dagger \hat{f}_d + E_{10}, \quad (14)$$

where $E_{10} \equiv -J_z S_a S_b + \frac{J_z(\Delta_1 - 1)}{2}(S_a + S_b) - |J_\perp| \sqrt{(\Delta_1^2 - 1) S_a S_b}$, $\epsilon_{1c} \equiv \frac{J_z(\Delta_1 - 1)}{2} S_a + \frac{J_z(\Delta_1 + 1)}{2} S_b - |J_\perp| \sqrt{(\Delta_1^2 - 1) S_a S_b}$, $\epsilon_{1d} \equiv \frac{J_z(\Delta_1 + 1)}{2} S_a + \frac{J_z(\Delta_1 - 1)}{2} S_b - |J_\perp| \sqrt{(\Delta_1^2 - 1) S_a S_b}$. Thus the energy spectrum is $E_A(n_c, n_d) = \epsilon_{1c} n_c + \epsilon_{1d} n_d + E_{10}$, where n_c and n_d are nonnegative integer numbers. For $J_z > |J_\perp|$, ϵ_{1c} and ϵ_{1d} are always positive; therefore the ground-state energy is $E_1(0, 0) = E_{10}$. When $J_z \rightarrow |J_\perp|$, $E_0(0, 0)$ approaches $-S_b(S_a + 1)$, which is the exact ground-state energy at $J_z = |J_\perp|$.

Like the original Hamilton (1), the effective Hamiltonian (12) also conserves the z component of the total spin. Therefore any of its eigenstates can be written as

$$|\psi_1(n_c, n_d)\rangle = \sum_m g_1(n_c, n_d, m) |S_a, m\rangle_a |S_b, S_z - m\rangle_b, \quad (15)$$

where $\max(-S_a, S_z - S_b) \leq m \leq \min(S_a, S_z + S_b)$, $g_1(n_c, n_d, m)$ is the expansion coefficient, and S_z is the total z component of the spin system. Using (13) and considering that $|\psi_1(n_c, n_d)\rangle$ is an eigenstate of both $\hat{f}_c^\dagger \hat{f}_c$ and $\hat{f}_d^\dagger \hat{f}_d$, with eigenvalues n_c and n_d respectively, we obtain

$$n_c - n_d = S_a - S_b - S_z. \quad (16)$$

For the ground state $|\psi_1(0, 0)\rangle$, $S_z = S_a - S_b$.

It is easy to find the ground state $|\psi_1(0, 0)\rangle$ of (12) from $\hat{f}_c |\psi_1(0, 0)\rangle = 0$,

$$|\psi_1(0,0)\rangle = D \sum_{m=S_a-2S_b}^{S_a} \left[-\text{sgn}(J_\perp) \sqrt{\frac{\Delta_1+1}{\Delta_1-1}} \right]^m |S_a, m\rangle_a |S_b, S_a - S_b - m\rangle_b, \quad (17)$$

$$= D \sum_{m=-S_b}^{S_b} \left[-\text{sgn}(J_\perp) \sqrt{\frac{\Delta_1+1}{\Delta_1-1}} \right]^{S_a-S_b-m} |S_a, S_a - S_b - m\rangle_a |S_b, m\rangle_b, \quad (18)$$

where $D \equiv \left[\frac{(\frac{\Delta_1+1}{\Delta_1-1})^{S_a-S_b} (\Delta_1+1)^{2S_b+1} - (\Delta_1-1)^{2S_b+1}}{2(\Delta_1^2-1)^{S_b}} \right]^{-1/2}$ is the normalization coefficient. When $J_\perp \rightarrow 0$, $|G_A\rangle \rightarrow |S_a, S_a\rangle_a |S_b, -S_b\rangle_b$, which is an exact ground state of the Hamiltonian (1) with $J_\perp = 0$ and $J_z > 0$.

The excited states of (12) can be obtained by the action

of \hat{f}_c^\dagger and \hat{f}_d^\dagger on the ground state $|\psi_1(0,0)\rangle$. With $S_a > S_b$, $\epsilon_{1c} < \epsilon_{1d}$, for a given S_z , the lowest excited state is $|\psi_1(n_c, 0)\rangle$ if $S_z < S_a - S_b$ and is $|\psi_1(0, n_d)\rangle$ if $S_z > S_a - S_b$. These two excited states can be written as

$$|\psi_1(n_c, 0)\rangle = D_c \exp(-i\zeta\pi\hat{S}_{az}) \sum_{n=0}^{n_c} \sum_{m=S_a-2S_b-n}^{S_a-n_c} (-1)^{m+n} \left(\sqrt{\frac{\Delta_1+1}{\Delta_1-1}} \right)^{m+2n} C_{n_c}^n \sqrt{C_{S_a-m}^{n_c}} |S_a, m\rangle_a |S_b, S_a - S_b - n_c - m\rangle_b, \quad (19)$$

$$|\psi_1(0, n_d)\rangle = D_d \exp(-i\zeta\pi\hat{S}_{az}) \sum_{m=S_a-2S_b+n_d}^{S_a} \left(-\sqrt{\frac{\Delta_1+1}{\Delta_1-1}} \right)^m \sqrt{C_{S_a+n_d-m}^{n_d}} |S_a, m\rangle_a |S_b, S_a - S_b + n_d - m\rangle_b, \quad (20)$$

where $\zeta = 0$ if $J_\perp > 0$ while $\zeta = 1$ if $J_\perp < 0$; D_c and D_d are the normalization constants, and C_n^m is the binomial coefficient.

Now we consider the ground state close to the other classical degenerate ground state $|S_a, -S_a\rangle_a |S_b, S_b\rangle_b$, in a way similar to the above. The Holstein-Primarkoff transformation is

$$\begin{aligned} \hat{S}'_{b-} &= \hat{f}_b^\dagger \sqrt{2S_b - \hat{f}_b^\dagger \hat{f}_b}, & \hat{S}'_{b+} &= \sqrt{2S_b - \hat{f}_b^\dagger \hat{f}_b} \hat{f}_b, \\ \hat{S}'_{bz} &= S_b - \hat{f}_b^\dagger \hat{f}_b, \\ \hat{S}'_{a-} &= \sqrt{2S_a - \hat{f}_a^\dagger \hat{f}_a} \hat{f}_a, & \hat{S}'_{a+} &= \hat{f}_a^\dagger \sqrt{2S_a - \hat{f}_a^\dagger \hat{f}_a}, \\ \hat{S}'_{az} &= \hat{f}_a^\dagger \hat{f}_a - S_a, \end{aligned} \quad (21)$$

where the bosonic operators f'_a and f'_b act on

$$|n'_a\rangle \equiv |S_a, -S_a + n'_a\rangle_a, \quad (22)$$

$$|n'_b\rangle \equiv |S_b, S_b - n'_b\rangle_b. \quad (23)$$

Thus one obtains a Hamiltonian

$$\begin{aligned} \hat{\mathcal{H}}'_A &\approx -J_z S_a S_b + J_z (S_b \hat{f}'_a \hat{f}'_a + S_a \hat{f}'_b \hat{f}'_b) \\ &+ J_\perp \sqrt{S_a S_b} (\hat{f}'_a \hat{f}'_b + \hat{f}'_b \hat{f}'_a), \\ &= \epsilon_{1c} \hat{f}'_c \hat{f}'_c + \epsilon_{1d} \hat{f}'_d \hat{f}'_d + E_{10}, \end{aligned}$$

where

$$\begin{aligned} \hat{f}'_c &= \sqrt{\frac{\Delta_1+1}{2}} \hat{f}'_a + \text{sgn}(J_\perp) \sqrt{\frac{\Delta_1-1}{2}} \hat{f}'_b, \\ \hat{f}'_d &= \text{sgn}(J_\perp) \sqrt{\frac{\Delta_1-1}{2}} \hat{f}'_a + \sqrt{\frac{\Delta_1+1}{2}} \hat{f}'_b. \end{aligned} \quad (24)$$

Therefore the eigenstates can be written as

$$|\psi'_1(n'_c, n'_d)\rangle = \sum_m g_1(n'_c, n'_d, m) |S_a, m\rangle_a |S_b, S_z - m\rangle_b, \quad (25)$$

with the constraint

$$n'_c - n'_d = S_a - S_b + S_z. \quad (26)$$

For the ground state $|\psi'_1(0,0)\rangle$, $S_z = S_b - S_a$.

$$|\psi'_1(0,0)\rangle = D' \sum_{m=-S_b}^{S_b} \left[-\text{sgn}(J_\perp) \sqrt{\frac{\Delta_1+1}{\Delta_1-1}} \right]^m |S_a, S_b - S_a - m\rangle_a |S_b, m\rangle_b, \quad (27)$$

where $D' \equiv \left[\frac{(\Delta_1+1)^{2S_b+1} - (\Delta_1-1)^{2S_b+1}}{2(\Delta_1^2-1)^{S_b}} \right]^{-1/2}$. When $J_\perp \rightarrow 0$, $|G_A\rangle \rightarrow |S_a, -S_a\rangle |S_b, S_b\rangle$, which is an exact ground state of the Hamiltonian (1) with $J_\perp = 0$ and $J_z > 0$.

The excited states of (24) can be obtained by the action of \hat{f}_c^\dagger and \hat{f}_d^\dagger on the ground state $|\psi'_1(0,0)\rangle$. With $S_a > S_b$, $\epsilon_{1c} < \epsilon_{1d}$, for a given S_z , the lowest excited state is $|\psi'_1(n'_c, 0)\rangle$ if $S_z > S_b - S_a$ and is $|\psi'_1(0, n'_d)\rangle$ if $S_z < S_b - S_a$. The explicit expressions of $|\psi'_1(n_c, 0)\rangle$ and $|\psi'_1(0, n_d)\rangle$ are like (19) and (20) for $|\psi_1(n_c, 0)\rangle$ and $|\psi_1(0, n_d)\rangle$, with $|S_a, m\rangle_a$, $|S_b, S_a - S_b - n_c - m\rangle_b$ and $|S_b, S_a - S_b + n_d - m\rangle_b$ replaced as $|S_a, -m\rangle_a$, $|S_b, -S_a + S_b + n_c + m\rangle_b$ and $|S_b, -S_a + S_b - n_d + m\rangle_b$, respectively.

It is important to note that $|\psi_1(0,0)\rangle$ and $|\psi'_1(0,0)\rangle$ are orthogonal unless $S_a = S_b$. Therefore, when $S_a \neq S_b$, the ground states are doubly degenerate ones $|\psi_1(0,0)\rangle$ and $|\psi'_1(0,0)\rangle$ at each parameter point in this regime.

When $S_a = S_b$, $\gamma \equiv \langle \psi_1(0,0) | \psi'_1(0,0) \rangle = \frac{2(2S_b+1)(\Delta_1^2-1)^{S_b}}{(\Delta_1+1)^{2S_b+1} - (\Delta_1-1)^{2S_b+1}}$; hence we must find the ground state in their two-dimensional subspace. Clearly $\langle \psi_1(0,0) | \hat{\mathcal{H}} | \psi_1(0,0) \rangle = \langle \psi'_1(0,0) | \hat{\mathcal{H}} | \psi'_1(0,0) \rangle \approx E_{10}$. $\langle \psi_1(0,0) | \hat{\mathcal{H}} | \psi'_1(0,0) \rangle = \langle \psi'_1(0,0) | \hat{\mathcal{H}} | \psi_1(0,0) \rangle \approx E_{10}\gamma$. Consequently, the ground state is found to be

$$|G_A(S_a = S_b)\rangle = \frac{1}{\sqrt{2}} [|\psi_1(0,0)\rangle + |\psi'_1(0,0)\rangle], \quad (28)$$

with energy $E_{10}(1 + \gamma)$. The energy of $\frac{1}{\sqrt{2}} [|\psi_1(0,0)\rangle - |\psi'_1(0,0)\rangle]$ is $E_{10}(1 - \gamma)$.

When J_\perp and J_z approach the boundary $J_z = -J_\perp > 0$ from the regime of $|G_A\rangle$, $|G_A\rangle$ approaches $e^{i\pi S_{az}} |S_a - S_b, \pm(S_a - S_b)\rangle$. When J_\perp and J_z approach the boundary $J_z = J_\perp > 0$ from the regime of $|G_A\rangle$, $|G_A\rangle$ approaches $|S_a - S_b, \pm(S_a - S_b)\rangle$.

B. $J_z < -|J_\perp|$

In this parameter regime, the classical ground states are $|S_a, S_a\rangle |S_b, S_b\rangle$, in which the two spins are both along the z direction, and $|S_a, -S_a\rangle |S_b, -S_b\rangle$, in which the two spins are both along the $-z$ direction.

Consider the ground state close to $|S_a, S_a\rangle_a |S_b, S_b\rangle_b$. We make the Holstein-Primarkoff transformation $\hat{S}_{\alpha-} = \hat{h}_\alpha^\dagger \sqrt{2S_\alpha - \hat{h}_\alpha^\dagger \hat{h}_\alpha}$, $\hat{S}_{\alpha+} = \sqrt{2S_\alpha - \hat{h}_\alpha^\dagger \hat{h}_\alpha} \hat{h}_\alpha$, $\hat{S}_{\alpha z} = S_\alpha - \hat{h}_\alpha^\dagger \hat{h}_\alpha$, where \hat{h}_α and \hat{h}_α^\dagger are bosonic operators, now with $|n_\alpha\rangle \equiv |S_\alpha, S_\alpha - n_\alpha\rangle_\alpha$, where $n_\alpha = 0, 1, \dots, 2S_\alpha$. When S_α is very large, $\langle \hat{h}_\alpha^\dagger \hat{h}_\alpha \rangle \ll 2S_\alpha$, $\hat{S}_{\alpha-} \approx (2S_\alpha)^{1/2} \hat{h}_\alpha^\dagger$, $\hat{S}_{\alpha z} \hat{S}_{\alpha z} \approx S_\alpha S_b - S_b \hat{h}_a^\dagger \hat{h}_a - S_a \hat{h}_b^\dagger \hat{h}_b$. Then the Hamiltonian (1) becomes

$$\hat{\mathcal{H}}_B = J_z S_a S_b - J_z (S_b \hat{h}_a^\dagger \hat{h}_a + S_a \hat{h}_b^\dagger \hat{h}_b) + J_\perp \sqrt{S_a S_b} (\hat{h}_a^\dagger \hat{h}_b + \hat{h}_b^\dagger \hat{h}_a). \quad (29)$$

We define another two bosonic operators,

$$\begin{aligned} \hat{h}_c &= -\text{sgn}(J_\perp) \sqrt{\frac{1-\Delta_2}{2}} \hat{h}_a + \sqrt{\frac{1+\Delta_2}{2}} \hat{h}_b, \\ \hat{h}_d &= \text{sgn}(J_\perp) \sqrt{\frac{1+\Delta_2}{2}} \hat{h}_a + \sqrt{\frac{1-\Delta_2}{2}} \hat{h}_b, \end{aligned} \quad (30)$$

where $\Delta_2 \equiv \frac{J_z(S_a - S_b)}{\sqrt{J_z^2(S_a - S_b)^2 + 4J_\perp^2 S_a S_b}}$. Then the Hamiltonian (1) becomes

$$\hat{\mathcal{H}}_B = \epsilon_{2c} \hat{h}_c^\dagger \hat{h}_c + \epsilon_{2d} \hat{h}_d^\dagger \hat{h}_d + E_{20}, \quad (31)$$

where $E_{20} \equiv J_z S_a S_b$, $\epsilon_{2c} \equiv -[\frac{J_z(1+\Delta_2)}{2} S_a + \frac{J_z(1-\Delta_2)}{2} S_b + |J_\perp| \sqrt{(1-\Delta_2^2) S_a S_b}]$, $\epsilon_{2d} \equiv -[\frac{J_z(1-\Delta_2)}{2} S_a + \frac{J_z(1+\Delta_2)}{2} S_b - |J_\perp| \sqrt{(1-\Delta_2^2) S_a S_b}]$. The energy spectrum is $E_B(n_c, n_d) = \epsilon_{2c} n_c + \epsilon_{2d} n_d + E_{20}$. Thus the ground state is $|S_a, S_a\rangle |S_b, S_b\rangle$.

The excited state $|\psi_2(n_c, n_d)\rangle$ of (29) can be obtained by the action of \hat{h}_c^\dagger and \hat{h}_d^\dagger on the ground state $|S_a, S_a\rangle |S_b, S_b\rangle$. It is obvious that ϵ_{2c} is always larger than ϵ_{2d} , for a given S_z , the lowest excited state is $|\psi_2(n_c, 0)\rangle$, with

$$n_c = S_a + S_b - S_z, \quad (32)$$

$$|\psi_2(n_c, 0)\rangle = D_{2c} \exp(-i\zeta \pi S_{az}) \sum_{m=\max(n_c-2S_b, 0)}^{n_c} \left(-\sqrt{\frac{1-\Delta_2}{1+\Delta_2}} \right)^m \sqrt{C_{n_c}^m} |S_a, S_a - m\rangle_a |S_b, S_b - n_c + m\rangle_b, \quad (33)$$

where $\zeta = 0$ if $J_\perp > 0$ while $\zeta = 1$ if $J_\perp < 0$,

and $D_{2c} = \left[\frac{(1+\Delta_2)^{n_c} (1-\Delta_2)^{n_0} - (1+\Delta_2)^{n_0-1} (1-\Delta_2)^{n_c+1}}{2\Delta_2(\Delta_2+1)^{n_c+n_0-1}} \right]^{-1/2}$,

where $n_0 = \max(n_c - 2S_b, 0)$.

Using the same method, we obtain the approximate Hamiltonian $\hat{\mathcal{H}}'_B$ close to the other classical ground state $|S_a, -S_a\rangle|S_b, -S_b\rangle$, which turns out to be the quantum ground state. The Holstein-Primarkoff transformation is now $\hat{S}_{\alpha+} = \hat{h}'_{\alpha\dagger}\sqrt{2S_{\alpha} - \hat{h}'_{\alpha\dagger}\hat{h}'_{\alpha}}$, $\hat{S}_{\alpha-} = \sqrt{2S_{\alpha} - \hat{h}'_{\alpha\dagger}\hat{h}'_{\alpha}}\hat{h}'_{\alpha}$, $\hat{S}_{\alpha z} = \hat{h}'_{\alpha\dagger}\hat{h}'_{\alpha} - S_{\alpha}$, where \hat{h}'_{α} and $\hat{h}'_{\alpha\dagger}$ are bosonic operators, with $|n'_{\alpha}\rangle \equiv |S_{\alpha}, n'_{\alpha} - S_{\alpha}\rangle_{\alpha}$. Thus we have Eqs. (29) to (31) with primed operators. In this set of eigenstates, the lowest excited states for a given S_z are $|\psi'_2(n'_c, 0)\rangle$, with

$$n'_c = S_z + S_a + S_b. \quad (34)$$

$|\psi'_2(n_c, 0)\rangle$ are like (33), with $|S_a, S_a - m\rangle_a$ and $|S_b, S_b - n_c + m\rangle_b$ replaced by $|S_a, -S_a + m\rangle_a$ and $|S_b, -S_b + n_c - m\rangle_b$.

$|\psi_2(0, 0)\rangle$ and $|\psi'_2(0, 0)\rangle$ are orthogonal, hence are just the doubly degenerate ground states in this regime, and can be written as

$$|G_B\rangle = |S_a + S_b, \pm(S_a + S_b)\rangle. \quad (35)$$

When J_{\perp} and J_z approach the boundary $J_z = J_{\perp} < 0$ from the regime of $|G_B\rangle$, $|G_B\rangle$ approaches $|S_a + S_b, \pm(S_a + S_b)\rangle$. When J_{\perp} and J_z approach the boundary $J_{\perp} = -J_z > 0$ from the regime of $|G_B\rangle$, $|G_B\rangle$ approaches $|S_a + S_b, \pm(S_a + S_b)\rangle$.

C. $J_{\perp} > |J_z|$

In this parameter regime, it is convenient to rewrite the Hamiltonian as

$$\mathcal{H} = J_{\perp}\sqrt{(S_a^2 - S_{az}^2)(S_b^2 - S_{bz}^2)}\cos(\varphi_a - \varphi_b) + J_z S_{az} S_{bz}, \quad (36)$$

where φ_{α} ($\alpha = a, b$) is the azimuthal angle.

In the vicinity of the classical ground state, $S_{az} \sim 0$, $S_{bz} \sim 0$, $\varphi_a - \varphi_b \sim \pi$, for simplicity we define $\varphi_a - \varphi_b = \varphi_{ab} + \pi$. Therefore

$$\begin{aligned} \mathcal{H}_C \approx & -J_{\perp}\sqrt{S_a S_b (S_a + 1)(S_b + 1)} + \frac{J_{\perp}^2 - J_z^2}{4(J_{\perp}\xi_+ - J_z)} S_z^2 \\ & + \frac{J_{\perp}\xi_+ - J_z}{4} (S_{2z} - \frac{J_{\perp}\xi_-}{J_{\perp}\xi_+ - J_z} S_{1z})^2 \\ & + 2J_{\perp}\sqrt{S_a S_b (S_a + 1)(S_b + 1)} (\frac{\varphi_{ab}}{2})^2, \end{aligned} \quad (37)$$

where $S_{2z} \equiv S_{az} - S_{bz}$, $\xi_+ \equiv \frac{1}{2}(\frac{S_a}{S_b} + \frac{S_b}{S_a})$, $\xi_- \equiv \frac{1}{2}(\frac{S_a}{S_b} - \frac{S_b}{S_a})$.

S_z commutes with \mathcal{H} , and is thus a constant of motion. Then $\hat{P}_2 \equiv \hat{S}_{2z} - \frac{J_{\perp}\xi_-}{J_{\perp}\xi_+ - J_z} \hat{S}_z$ and $\hat{X}_2 \equiv \hat{\varphi}_{ab}/2$ are conjugate variables, as $\hat{S}_{\alpha z}$ and $\hat{\varphi}_{\alpha}$ are canonically conjugate variables. The Hamiltonian is then similar to that of a

harmonic oscillator. The energy spectrum is thus

$$\begin{aligned} E_3(n, S_z) = & -J_{\perp}\sqrt{S_a S_b (S_a + 1)(S_b + 1)} \\ & + \frac{J_{\perp}^2 - J_z^2}{4(J_{\perp}\xi_+ - J_z)} S_z^2 \\ & + (n + \frac{1}{2})\sqrt{2J_{\perp}(J_{\perp}\xi_+ - J_z)}\sqrt{S_a(S_a + 1)S_b(S_b + 1)} \\ \approx & -J_{\perp}\sqrt{S_a S_b (S_a + 1)(S_b + 1)} + \frac{J_{\perp}^2 - J_z^2}{4(J_{\perp}\xi_+ - J_z)} S_z^2 \\ & + (n + \frac{1}{2})\sqrt{2J_{\perp}(J_{\perp}\xi_+ - J_z)} S_a S_b, \end{aligned} \quad (38)$$

where n is the quantum number of the harmonic oscillator. The eigenstate for $n = 0$ can be written as

$$|\psi_3(0, S_z)\rangle = Z(S_z) \sum_m f(m, S_z) |S_a, m\rangle_a |S_b, S_z - m\rangle_b, \quad (39)$$

where $f(m, S_z) = (-1)^m \exp[-\sqrt{\frac{J_{\perp}\xi_+ - J_z}{2J_{\perp}S_a S_b}} m(m - \frac{J_{\perp}\xi_+ - J_z}{J_{\perp}\xi_+ - J_z} S_z)]$, with $\max(-S_a, S_z - S_b) \leq m \leq \min(S_a, S_z + S_b)$; $Z(S_z) \equiv \frac{1}{\sqrt{\sum_m |f(m, S_z)|^2}}$ is the normalization coefficient.

The ground state is thus

$$|G_C\rangle = |\psi_3(0, p)\rangle = Z(p) \sum f(m, p) |S_a, m\rangle_a |S_b, p - m\rangle_b, \quad (40)$$

where $p = 0$ if $S_a - S_b$ is an integer, while $p = \pm 1/2$ if $S_a - S_b$ is a half integer.

For $S_a = S_b = S$ and $J_{\perp} \gg J_z$, we have calculated the entanglement entropy of $|G_C\rangle$,

$$\mathcal{E}(|G_C\rangle) = -\sum [Z(p)f(m, p)]^2 \log_{2S+1} [Z(p)f(m, p)]^2. \quad (41)$$

It is evaluated that when $S \rightarrow \infty$, $\mathcal{E}(|G_C\rangle) \approx 1/2$, which is very large.

When J_{\perp} and J_z approach the boundary $J_z = J_{\perp} > 0$ from the regime of $|G_C\rangle$, it approaches $|S_a - S_b, p\rangle$, where $p = 0$ if $S_a - S_b$ is an integer while $p = \pm 1/2$ if $S_a - S_b$ is a half integer. When J_{\perp} and J_z approach the boundary $J_z = -J_{\perp} < 0$ from the regime of $|G_C\rangle$, it approaches $e^{i\pi S_{az}} |S_a + S_b, p\rangle$.

D. $J_{\perp} < -|J_z|$

The energy spectrum for $J_{\perp} < 0$ can be obtained by using $\mathcal{H}(J_{\perp}, J_z) = U\mathcal{H}(-J_{\perp}, J_z)U^{\dagger}$, where $U \equiv e^{i\pi S_{az}}$. Therefore, in the regime $J_{\perp} < -|J_z|$, the energy spectrum is also given by Eq. (38).

The ground state is thus

$$\begin{aligned} |G_D\rangle = & U|G_C\rangle \\ = & Z(p) \sum |f(m, p)| |S_a, m\rangle |S_b, p - m\rangle, \end{aligned} \quad (42)$$

with $\max(-S_a, S_z - S_b) \leq m \leq \min(S_a, S_z + S_b)$.

Obviously the entanglement entropy of $|G_D\rangle$ is the same as that of $|G_C\rangle$, with J_\perp reversing its sign.

When J_\perp and J_z approach the boundary $J_z = -J_\perp > 0$ from the regime of $|G_D\rangle$, it approaches $e^{i\pi S_{az}}|S_a - S_b, p\rangle$. When J_\perp and J_z approach the boundary $J_z = J_\perp < 0$ from the regime of $|G_D\rangle$, it approaches $|S_a + S_b, p\rangle$.

E. The ground states on the four parameter boundaries

When $J_z = J_\perp > 0$, the Hamiltonian (1) is $\mathcal{H} = J_z \hat{S}_a \cdot \hat{S}_b$, the degenerate ground states are $|S_a - S_b, S_z\rangle = \sum_m g(S_a - S_b, S_z, m) |S_a, m\rangle |S_b, S_z - m\rangle$, with $S_z = S_b - S_a, \dots, S_a - S_b$. Here $g(S_a - S_b, S_z, m)$ is the Clebsch-Gordan coefficient.

When $J_z = -J_\perp > 0$, the degenerate ground states are $e^{i\pi \hat{S}_{az}} |S_a - S_b, S_z\rangle = \sum_m (-1)^m g(S_a - S_b, S_z, m) |S_a, m\rangle |S_b, S_z - m\rangle$, with $S_z = S_b - S_a, \dots, S_a - S_b$.

When $J_z = J_\perp < 0$, the ground states are $|S_a + S_b, S_z\rangle = \sum_m g(S_a + S_b, S_z, m) |S_a, m\rangle |S_b, S_z - m\rangle$, with $S_z = -S_a - S_b, \dots, S_a + S_b$.

When $J_z = -J_\perp < 0$, the ground states are $e^{i\pi \hat{S}_{az}} |S_a + S_b, S_z\rangle = \sum_m (-1)^m g(S_a + S_b, S_z, m) |S_a, m\rangle |S_b, S_z - m\rangle$, with $S_z = -S_a - S_b, \dots, S_a + S_b$.

The boundaries are where quantum phase transition take place. We have known that the ground states $|G_A\rangle$, $|G_B\rangle$, $|G_C\rangle$, $|G_D\rangle$, in the four regimes discussed in previous subsections, depend on the values of J_z and J_\perp . Starting as a ground state in one of these regimes (see FIG. 8), when J_z and J_\perp adiabatically approach each boundary regime, the ground state always approaches one of the degenerate ground states on the boundary. In entering the other regime across the boundary, the ground state restarts from another one of the degenerate ground states on the boundary.

F. Comparison with the numerical results

As each eigenstate for $J_\perp < 0$ can be obtained by acting $e^{i\pi \hat{S}_{az}}$ on an eigenstate for $J_\perp = |J_\perp|$, we only need to consider the half of the parameter space with $J_\perp \geq 0$.

In this half parameter space, We have calculated the dependence of the entanglement on $1/\eta \equiv J_z/J_\perp$, using the ground states analytically obtained above in regimes A, C, and B. We compare these analytical results with the numerical results. The reason of choosing $1/\eta$ rather than η is because $J_z = 0$ in the middle of the half parameter space. In this half parameter space, regime B is $1/\eta < -1$, regime C is $-1 < 1/\eta < 1$, while regime A is $1/\eta > 1$.

Figure 9 shows the the entanglement in the ground states for different values of $S_a = S_b$ for $1/\eta > -1$. Ne-

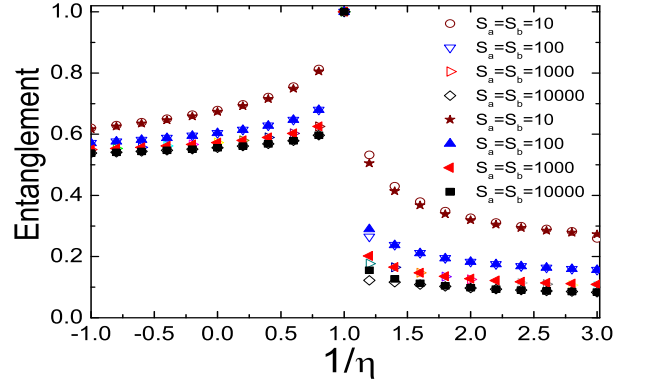


FIG. 9: (Color online) The entanglement entropy of the ground state as a function of $1/\eta \equiv J_z/J_\perp$. The filled symbols describe the analytical results. The empty symbols describe the numerical results.

glected is regime B, i.e. $1/\eta < -1$, as the ground state is exactly $|S_a, S_a\rangle |S_b, S_b\rangle$ or $|S_a, -S_a\rangle |S_b, -S_b\rangle$, without entanglement. Figure 9 clearly indicates excellent fitting between the analytical results in this section and the numerical results.

Excellent fitting between our analytical results and the numerical results are also obtained for excited states. We have calculated the lowest energy states of different values of S_z for $S_a = 12000$ and $S_b = 10000$. Figure 10 shows the the regime $1/\eta > -1$, i.e., regimes C and A, while Fig.11 shows the regime $1/\eta < -1$, i.e., regime B. The reason for this separation is that the low-energy excited state in regime B is with large magnitudes of S_z , while those in regimes C and A are with small magnitudes of S_z .

In conclusion, our analytical results fit the numerical results very well.

IX. SUMMARY

In this paper, we considered a binary mixture of two species of pseudo-spin- $\frac{1}{2}$ atoms with interspecies spin exchange in the absence of an external potential, and extended the study of its ground states to the whole parameter space of the two effective spin coupling strengths. Meanwhile, this provides a model of studying the relation between the classical model and quantum ground states.

We first analyzed the corresponding classical Hamiltonian. We found the fixed points of the classical dynamics, and discussed their stability situation both analytically and numerically. The bifurcations were discussed.

The classical evolution can be reproduced in quantum dynamics if starting from an initial state which is disentangled between the two species, as we have demonstrated.

In the case that the atom numbers of the two species

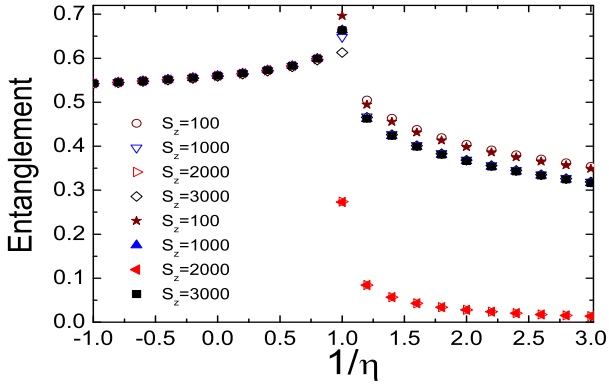


FIG. 10: (Color online) The entanglement entropy of the lowest energy excited states for different values of S_z under $S_a = 12000$ and $S_b = 10000$, as a function $1/\eta = J_z/J_\perp$. Here we show the regime $\eta > -1$, in which the low-energy excited states are with small magnitudes of S_z . The filled symbols describe the analytical results. The empty symbols describe the numerical results.

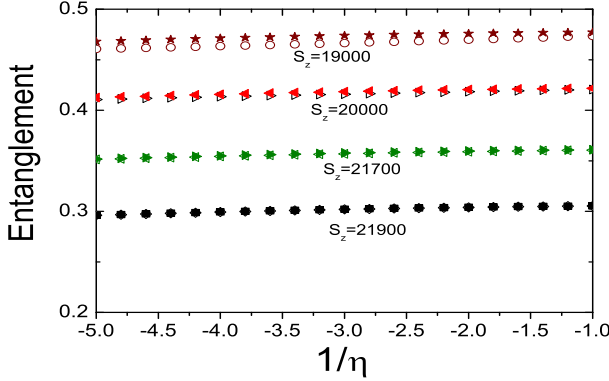


FIG. 11: (Color online) The entanglement entropy of the quantum states as a function $1/\eta = J_\perp/J_z$, for different values of S_z under $S_a = 12000$ and $S_b = 10000$ in regime B ($1/\eta < -1$), where the low energy excited states have large magnitudes of S_z . The filled symbols describe the analytical results. The empty symbols describe the numerical results.

are equal, we confirmed in our system the previous claim that a classical fixed point bifurcation corresponds to maximal entanglement in the quantum ground state. Moreover, we find the result that when the two atom numbers are unequal, the entanglement of the quantum ground state at the parameter point of the bifurcation is not maximal, while the state corresponding to the fixed point that bifurcates indeed possesses maximal entanglement at that parameter point.

A quantum ground state can be regarded as the classical ground state with quantum fluctuations. This perspective leads to solutions of the ground states in all parameter regimes, by obtaining an effective Hamiltonian near each classical ground state. Using entanglement en-

tropy as the quantity characterizing the ground states, we find that the analytical results fit the numerical results very well. We have made many detailed discussions.

Our work establishes EBEC as a system manifesting connections between classical dynamics and quantum behavior.

Acknowledgments

We thank Li Ge and Bailin Hao for useful discussion. This work was supported by the National Science Foundation of China (Grant No. 11074048) and the Ministry of Science and Technology of China (Grant No. 2009CB929204).

Appendix: Classical fixed points

For our problem, the desired Lyapunov function will always be found by defining

$$\mathcal{L} = \gamma_1 \mathcal{H} + \gamma_2 J_z (S_{az} + S_{bz})^2 \quad (\text{A.1})$$

where γ_1 and γ_2 are suitably chosen coefficients. It is clear that $\frac{d\mathcal{L}}{dt} = 0$.

We find the following fixed points specified by the values of $\mathbf{S}_\alpha = S_\alpha \mathbf{n}_\alpha$, where $\mathbf{n}_\alpha \equiv (\sin \theta_\alpha \cos \varphi_\alpha, \sin \theta_\alpha \sin \varphi_\alpha, \cos \theta_\alpha)$, $0 \leq \theta_\alpha \leq \pi$, $0 \leq \varphi_\alpha < 2\pi$, $\alpha = a, b$.

(1) $\mathbf{n}_a = -\mathbf{n}_b = (0, 0, \pm 1)$; that is, one spin is parallel to the z direction, the other is antiparallel to the z direction. At these two points the eigenvalues of \mathcal{J} are $\mu_1 = \mu_2 = 0$, $\mu_{3,4} = \pm \sqrt{\frac{\zeta_3 - \zeta_4}{2}}$, $\mu_{5,6} = \pm \sqrt{\frac{\zeta_3 + \zeta_4}{2}}$, where $\zeta_3 \equiv 2J_\perp^2 S_a S_b - J_z^2 (S_a^2 + S_b^2)$, $\zeta_4 = J_z (S_a - S_b) \sqrt{J_z^2 (S_a + S_b)^2 - 4J_\perp^2 S_a S_b}$. If we define $\eta_1 = \frac{1}{2} \left(\sqrt{\frac{S_a}{S_b}} + \sqrt{\frac{S_b}{S_a}} \right)$, when $\eta_1 |J_z| < |J_\perp|$, there are eigenvalues with positive real part, and these two fixed points are unstable. Otherwise, the stabilization cannot be judged by the eigenvalues. One finds the Lyapunov function $\mathcal{L} = \mathcal{H} - \frac{J_z}{4} (S_{az} + S_{bz})^2$, which is minimal for $J_z > 0$ (or maximal for $J_z < 0$) at each of these two fixed points in the parameter region $\eta_1 |J_z| > |J_\perp|$, where each of these two fixed points is thus stable.

(2) $\mathbf{n}_a = -\mathbf{n}_b = (\cos \varphi, \sin \varphi, 0)$, where $0 \leq \varphi < 2\pi$. The two spins are antiparallel and both are on the $x-y$ plane. At this point, the eigenvalues of \mathcal{J} are $\mu_1 = \mu_2 = \mu_3 = \mu_4 = 0$, $\mu_{5,6} = \pm \sqrt{2J_\perp J_z S_a S_b - J_\perp^2 (S_a^2 + S_b^2)}$. If we define $\eta_2 = \frac{2S_a S_b}{S_a^2 + S_b^2}$, when $0 < J_\perp < \eta_2 J_z$ or $\eta_2 J_z < J_\perp < 0$, some eigenvalues have positive real part, hence this fixed point is unstable. When $J_\perp > \eta_2 J_z \geq 0$ or $J_\perp < \eta_2 J_z \leq 0$, one finds the Lyapunov function $\mathcal{L} = \mathcal{H} + \gamma_2 J_z (S_{az} + S_{bz})^2$, which is minimal at the fixed point as $\gamma_2 \rightarrow \infty$. When $J_z J_\perp < 0$, one finds that $\mathcal{L} = -\mathcal{H} + \gamma_2 J_z (S_{az} + S_{bz})^2$ is minimal at the fixed point as $\gamma_2 \rightarrow \infty$.

TABLE I: Stable regimes of the fixed points. $\eta_1 \equiv \frac{1}{2} \left(\sqrt{\frac{S_a}{S_b}} + \sqrt{\frac{S_b}{S_a}} \right)$, $\eta_2 \equiv \frac{2S_a S_b}{S_a^2 + S_b^2}$.

No.	Fixed Points	Stable regions
1	$\mathbf{n}_a = -\mathbf{n}_b = (0, 0, \pm 1)$	$\eta_1 J_z > J_\perp $
2	$\mathbf{n}_a = -\mathbf{n}_b = (\cos \varphi, \sin \varphi, 0)$	$J_\perp > 0, J_\perp > \eta_2 J_z$ or $J_\perp < 0, J_\perp < \eta_2 J_z$
3	$\mathbf{n}_a = \mathbf{n}_b = (\cos \varphi, \sin \varphi, 0)$	$J_\perp > 0, J_\perp > -\eta_2 J_z$ or $J_\perp < 0, J_\perp < -\eta_2 J_z$
4	$\mathbf{n}_a = \mathbf{n}_b = (0, 0, \pm 1)$	All
5	$\mathbf{n}_a = -\mathbf{n}_b$	$J_\perp = J_z$
6	$\mathbf{n}_a = \mathbf{n}_b$	$J_\perp = J_z$
7	$\mathbf{n}_a = (\sin \theta \cos \varphi, \sin \theta \sin \varphi, \cos \theta)$, $\mathbf{n}_b = (\sin \theta \cos \varphi, \sin \theta \sin \varphi, -\cos \theta)$	$J_\perp = -J_z$
8	$\mathbf{n}_a = (\sin \theta \cos \varphi, \sin \theta \sin \varphi, \cos \theta)$, $\mathbf{n}_b = (-\sin \theta \cos \varphi, -\sin \theta \sin \varphi, \cos \theta)$	$J_\perp = -J_z$

Thus this fixed point is stable if $J_\perp > 0, J_\perp > \eta_2 J_z$ or $J_\perp < 0, J_\perp < \eta_2 J_z$.

(3) $\mathbf{n}_a = \mathbf{n}_b = (\cos \varphi, \sin \varphi, 0)$; that is, the two spins are parallel and on the $x - y$ plane. At this point, the eigenvalues of \mathcal{J} are $\mu_1 = \mu_2 = \mu_3 = \mu_4 = 0$, $\mu_{5,6} = \pm \sqrt{-J_\perp^2 (S_a^2 + S_b^2) - 2J_\perp J_z S_a S_b}$. When $-\eta_2 J_z < J_\perp < 0$ or $0 < J_\perp < \eta_2 J_z$, some eigenvalues have positive real parts, hence the fixed point is unstable. For $J_\perp J_z > 0$, one finds $\mathcal{L} = -\mathcal{H} + \gamma_2 J_z (S_{az} + S_{bz})^2$ is minimal at the fixed point as $\gamma_2 \rightarrow \infty$. For $J_\perp J_z < 0$ one finds $\mathcal{L} = \mathcal{H} + \gamma_2 J_z (S_{az} + S_{bz})^2$, which is minimal at the fixed point as $\gamma_2 \rightarrow \infty$. Therefore the fixed point is stable when $J_\perp > 0, J_\perp > -\eta_2 J_z$ or $J_\perp < 0, J_\perp < \eta_2 J_z$.

(4) $\mathbf{n}_a = \mathbf{n}_b = (0, 0, \pm 1)$; that is, the two spins are both parallel or antiparallel to the z direction. At each of these two fixed points, the eigenvalues of \mathcal{J} are $\mu_1 = \mu_2 = 0$, $\mu_{3,4} = \pm \sqrt{\frac{\zeta_1 - \zeta_2}{2}}$, $\mu_{5,6} = \pm \sqrt{\frac{\zeta_1 + \zeta_2}{2}}$; here $\zeta_1 \equiv -2J_\perp^2 S_a S_b - J_z^2 (S_a^2 + S_b^2)$, $\zeta_2 \equiv J_z (S_a + S_b) \sqrt{J_z^2 (S_a - S_b)^2 + 4J_\perp^2 S_a S_b}$. The stabilization cannot be judged by the eigenvalues. But one finds the Lyapunov function $\mathcal{L} = -(S_{az} + S_{bz})^2$, which is minimal at the fixed point. Hence these two fixed points are always stable.

(5) In case $J_\perp = J_z$, the solution $\mathbf{n}_a = \mathbf{n}_b$ with any possible is a fixed point; that is, the two spins are always

parallel. The Lyapunov function $\mathcal{L} = -\mathbf{S}_a \cdot \mathbf{S}_b$ is minimal here, thus this fixed point is stable.

(6) In case $J_\perp = J_z$, the solution $\mathbf{n}_a = -\mathbf{n}_b$ with any possible is a fixed point; that is, the two spins are always antiparallel. The Lyapunov function $\mathcal{L} = \mathbf{S}_a \cdot \mathbf{S}_b$ is minimal here, thus this fixed point is stable.

(7) In case $J_\perp = -J_z$, $\mathbf{n}_a = (\sin \theta \cos \varphi, \sin \theta \sin \varphi, \cos \theta)$ while $\mathbf{n}_b = (\sin \theta \cos \varphi, \sin \theta \sin \varphi, -\cos \theta)$ is a fixed point; that is, the z components of the two spins are opposite. One finds a Lyapunov function $\mathcal{L} = -\mathbf{S}_a \cdot \mathbf{S}'_b$, where $\mathbf{S}'_b = (S_b \sin \theta \cos \varphi, S_b \sin \theta \sin \varphi, S_b \cos \theta)$, which is minimal at this fixed point. Thus this fixed point is stable.

(8) In case $J_\perp = -J_z$, $\mathbf{n}_a = (\sin \theta \cos \varphi, \sin \theta \sin \varphi, \cos \theta)$ while $\mathbf{n}_b = (-\sin \theta \cos \varphi, -\sin \theta \sin \varphi, \cos \theta)$ is a fixed point; that is, the x and y components of the two spins are opposite. One finds a Lyapunov function $\mathcal{L} = \mathbf{S}_a \cdot \mathbf{S}''_b$, where $\mathbf{S}''_b = (-S_b \sin \theta \cos \varphi, -S_b \sin \theta \sin \varphi, -S_b \cos \theta)$, which is minimal at this fixed point. Thus this fixed point is stable.

All of the fixed points and their stable regimes are listed in Table I.

-
- [1] S. Schneider and G. J. Milburn, *Phys. Rev. A* **65**, 042107 (2002).
[2] M. C. Nemes et al., *Phys. Lett. A* **354**, 60 (2006).
[3] A. P. Hines, R. H. McKenzie, and G. J. Milburn, *Phys. Rev. A* **71**, 042303 (2005).
[4] X. W. Hou, J. H. Chen, B. Hu, *Phys. Rev. A* **71**, 034302 (2005).
[5] M. E. Kellman and V. Tyng, *Phys. Rev. A* **66**, 013602 (2002).
[6] Q. Xie and W. Hai, *Euro. Phys. J. D* **39**, 277 (2006).
[7] G. Santos, A. Tonel, A. Foerster, and J. Links, *Phys. Rev. A* **73**, 023609 (2006).
[8] G. Santos, A. Foerster, J. Links, E. Mattei, and S. R. Dahmen, *Phys. Rev. A* **81**, 063621 (2010).
[9] T. Zibold, E. Nicklas, C. Gross, and M. K. Oberthaler, *Phys. Rev. Lett.* **105**, 204101 (2010).
[10] S. Chaudhury, A. Smith, B. E. Anderson, S. Ghose and P. S. Jessen, *Nature (London)* **461**, 768 (2009).
[11] Y. Shi, *Int. J. Mod. Phys. B* **15**, 3007 (2001).
[12] Y. Shi and Q. Niu, *Phys. Rev. Lett.* **96**, 140401 (2006).
[13] Y. Shi, *Europhys. Lett.* **86**, 60008 (2009).
[14] Y. Shi, *Phys. Rev. A* **82**, 013637 (2010).
[15] R. Wu and Y. Shi, *Phys. Rev. A* **83**, 025601 (2011).
[16] T. Holstein, H. Primakoff, *Phys. Rev.* **58**, 1098 (1940).